

Study on the crystal and electronic structure of $\text{Y}_{1-x}\text{Pr}_x\text{Ba}_2\text{Cu}_3\text{O}_{7-y}$ ceramics

This article has been downloaded from IOPscience. Please scroll down to see the full text article.

1998 J. Phys.: Condens. Matter 10 7015

(<http://iopscience.iop.org/0953-8984/10/31/017>)

View [the table of contents for this issue](#), or go to the [journal homepage](#) for more

Download details:

IP Address: 171.66.16.209

The article was downloaded on 14/05/2010 at 16:39

Please note that [terms and conditions apply](#).

Study on the crystal and electronic structure of $Y_{1-x}Pr_xBa_2Cu_3O_{7-y}$ ceramics

Shi Lei[†], Huang Yunsong[†], Jia Yunbo[†], Liu Xianming[†], Zhou Guien[†] and Zhang Yuheng^{†‡}

[†] Structure Research Laboratory, University of Science and Technology of China, Hefei, Anhui 230026, People's Republic of China

[‡] CCAST, World Laboratory, Beijing 100080, People's Republic of China

Received 10 February 1998

Abstract. $PrBa_2Cu_3O_{7-y}$ (PrBCO) is unique in the $RBa_2Cu_3O_{7-y}$ ($R =$ rare earth) series because it is not superconducting. In fact, for $Y_{1-x}Pr_xBa_2Cu_3O_{7-y}$, T_c drops monotonically with Pr concentration, with T_c going to zero at 55% Pr. There have been many studies of this material with the hope that an explanation for the lack of superconductivity in PrBCO might help explain why $YBa_2Cu_3O_{7-y}$ is superconducting. Unfortunately, to date, none of the proposed explanations has been totally satisfactory and without objection due to the considerable controversy of the results obtained by different experiments. In this paper, a series of samples of $Y_{1-x}Pr_xBa_2Cu_3O_{7-y}$ (YPrBCO) ($0 \leq x \leq 0.55$) have been studied by x-ray diffraction, Raman spectroscopy and XPS. The results reveal that the Pr dopant does not change the orthorhombic symmetry of the samples. The peak positions at 502 and 334 cm^{-1} of the Raman spectra become shifted for different Pr concentration, which suggests a change in oxygen content upon substitution of Pr ion for Y ion. There are two valences of Pr ions in YPrBCO. The valence of Pr is changed with change in Pr content x . The relative content of Pr^{3+} and Pr^{4+} is closely related to the total Pr content x . The valence of Pr is close to $3+$ for small x , and is increased as x increases. The valence change of the Pr ion would directly result in the increase of oxygen content. A ligand hole localized on the Pr–O(2)/O(3) band would remove a hole from the conduction band and yield a formal Pr^{4+} site. The strong hybridization between Pr 4f electrons and conduction holes in the CuO_2 planes induces a localization of mobile holes causing the suppression of superconductivity in the YPrBCO system. In addition, the existence of some extra oxygen atoms around Pr will also affect the distortion of the CuO_2 planes and possibly assist in the suppression of the superconductivity.

1. Introduction

It is well known that different rare-earth ions (except Pr, Ce and Tb) can be substituted in place of yttrium ions in $YBa_2Cu_3O_{7-y}$ (YBCO), giving superconductivity with nearly the same critical temperature $T_c = 90$ K. Ce and Tb yield the stable perovskites $BaCeO_3$ and $BaTbO_3$ rather than the $YBa_2Cu_3O_7$ -type structure. The Pr element is the only one which is isostructural with YBCO but is not a high- T_c superconductor. As the Pr concentration is increased in $Y_{1-x}Pr_xBa_2Cu_3O_{7-y}$ (YPrBCO) T_c is monotonically decreasing, with superconductivity vanishing at a concentration of $x \approx 0.55$ [1–3]. The normal-state electrical behaviour also undergoes a transition from metallic (for $x \leq 0.55$) to semiconducting (for $x \geq 0.55$) at roughly the same concentration. There have been many studies of this material with the hope that an explanation for the lack of superconductivity in YPrBCO might help explain why YBCO is superconducting. The mechanisms proposed

to explain both the suppression of superconductivity and the occurrence of semiconductivity can be distinguished according to the valence of Pr ions assumed. The idea of hole filling in the CuO_2 planes requires tetravalence or mixed valence [4, 5]. The alternative mechanisms are mediated by the hybridization of the 4f electrons of Pr^{3+} with O 2p–Cu 3d electrons in the CuO_2 planes [5–8]. Hybridization is supposed to lead to either Abrikosov–Gorov-type pair breaking and/or localization of holes in the CuO_2 planes. Unfortunately, none of these proposed explanations alone has been totally satisfactory and without objections due to the considerable controversy of Pr valence obtained by different experiments. Evidence from electron-energy-loss spectroscopy (EELS) [9] and x-ray absorption spectroscopy [10–12] indicates that the valence of Pr is close to 3+. However, the measured results of magnetic susceptibility [5, 6, 15], specific heat [6, 7, 13, 14] and Hall effect [15] suggest that the valence of Pr is 4+.

X-ray diffraction (XRD) and Raman spectrum analyses are useful tools for the determination of crystal structure and the checking of impurities. XRD results show that YPrBCO is isostructural with YBCO. The first Raman measurements on the YPrBCO system were made by Bhadra *et al* [16] who studied the system for x up to 0.5 and for pure PrBCO. They noted that the 500 cm^{-1} mode hardened as Pr was added. On the other hand, photoemission techniques obviously have the potential to provide direct insight into the involvement of Pr 4f states in the band structures of the Pr-doped YBCO system. In fact, there have been previous studies of the system $\text{Y}_{1-x}\text{Pr}_x\text{Ba}_2\text{Cu}_3\text{O}_y$ by several groups using the x-ray photoemission spectrum [17–20]. The most significant feature of the latter experiments was a shift to high binding energy in the leading edge of Ba core level peaks with increasing Pr doping. A similar shift was observed upon increasing y in $\text{YBa}_2\text{Cu}_3\text{O}_{7-y}$. However, the other core levels (O 1s, Y 3d, Cu 2p) showed no systematic change in lineshape or binding energy with Pr doping. In any case, the problem of the Pr valence in Pr-doped YBCO ceramics is still unresolved due to the overlap of the Pr 3d core line with the Cu 2p core line. In this paper, the XRD, Raman spectrum, x-ray photoemission spectrum (XPS) and a spectrum-extraction technique are applied to check the crystal structure and the electronic structure in Pr-doped YBCO ceramics.

2. Experiment

Samples of $\text{Y}_{1-x}\text{Pr}_x\text{Ba}_2\text{Cu}_3\text{O}_{7-y}$ with $x = 0, 0.05, 0.1, 0.2, 0.4$ and 0.55 were prepared by the conventional solid-state reaction technique. Appropriate amounts of high purity Y_2O_3 , Pr_6O_{11} , BaCO_3 and CuO were mixed and calcined at 890°C in air for 24 h. After intermediate grinding, they were reheated to 890°C for another 24 h. The same process was repeated at least twice in order to make the samples homogeneous. Then they were pressed into pellets and sintered at 920°C for 24 h in flowing oxygen. Subsequently, the pellets were slowly cooled to room temperature at 2°C min^{-1} in flowing oxygen. A.C. susceptibility measurements give the same results as those reported by Neumeier [21] which reveal that the superconducting transition temperature T_c decreases monotonically with increasing Pr content x and for $x \approx 0.55$ no transition to a superconducting phase is observed.

XRD analysis was carried out using a Rigaku D/max-rA diffractometer with graphite monochromatized Cu $K\alpha$ radiation. Raman spectrum experiments were conducted using a Spex-1403 spectrometer with a back-reflection geometric layout. The excitation source was argon laser operating at 5145 \AA . The XPS study was carried out on a VG ESCALAB MK-II electron spectrometer. The clean surfaces of the samples were obtained by scraping them *in situ* with a diamond file in ultrahigh vacuum. The base pressure in the vacuum system was about 1×10^{-9} mbar. A magnesium anode provided the x-ray radiation

(Mg $K\alpha = 1253.6$ eV) for excitation. All the measurements were carried out at room temperature.

3. Results and discussion

3.1. XRD analyses for the samples $Y_{1-x}Pr_xBa_2Cu_3O_{7-y}$ ($0 \leq x \leq 0.55$)

Figure 1(a) shows the XRD patterns of the $Y_{1-x}Pr_xBa_2Cu_3O_{7-y}$ ($x = 0.0, 0.05, 0.1, 0.2, 0.4, 0.55$). From these XRD patterns, first, it can be noted that Pr dopant does not change the orthorhombic symmetry of the samples. The samples do not contain any impurity and belong to the ideal pure Y-123 single phase. Secondly, figure 1(a) reflects the fact that the position of typical diffraction peaks of Y-123 phase changes successively with the increase of Pr content and suggests that the unit-cell parameters of the Pr-doped Y-123 phase vary correspondingly, as shown in figure 1(b) (obtained from a least-squares refinement). Figure 1(b) shows that a , b and c axes monotonically increase with the increase of Pr content, as reported by Neumeier [21]. Since the ionic radius of Pr (1.16 Å for Pr^{3+} and 1.00 Å for Pr^{4+}) is larger than that of Y (= 0.95 Å), the increase of lattice parameters means that most of the Pr substitutes onto the Y site and is well ordered with respect to the unit cell.

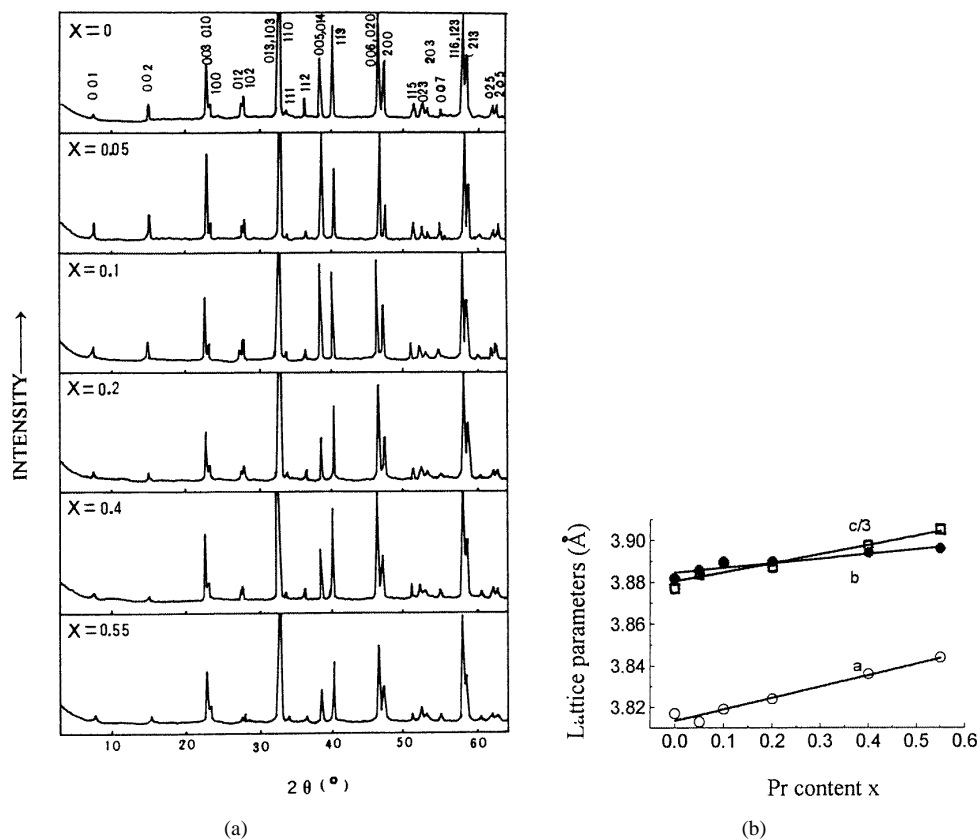


Figure 1. (a) XRD patterns of the samples $Y_{1-x}Pr_xBa_2Cu_3O_{7-y}$; (b) the change of the lattice parameters a , b and c dependent on the Pr content x , obtained by a least-squares refinement.

3.2. Analyses of Raman spectra for the samples $Y_{1-x}Pr_xBa_2Cu_3O_{7-y}$ ($0 \leq x \leq 0.55$)

Usually, Raman spectra in the range from 100 to 700 cm^{-1} show the vibrations of Ba, Cu and oxygen and are highly sensitive to the existence of an impurity phase in the $YBa_2Cu_3O_{7-y}$ system. Figure 2(a) shows the Raman spectra for the samples $Y_{1-x}Pr_xBa_2Cu_3O_{7-y}$ ($x = 0.0, 0.2, 0.4, 0.55$). It can be seen that the peaks of the Raman spectra appear at 154, 334 and 502 cm^{-1} , besides the sharp lines below 150 cm^{-1} which may be due to laser plasma lines and the Raman spectrum of air [22]. The characteristic lines at 154, 334 and 502 cm^{-1} have been identified as modes having A_g symmetry lattice vibrations for the superconducting phase $YBa_2Cu_3O_{7-y}$ [22–24] suggesting that the samples are the ideal pure Y-123 phase, which agrees with the XRD results. The curves of the line positions of 334 and 502 cm^{-1} peaks dependent on Pr content are shown in figure 2(b). As seen in figure 2(b), the peak position at 502 cm^{-1} is a little shifted to a higher frequency while the peak position at 334 cm^{-1} is shifted to lower frequency with the increase of Pr content. Radousky *et al* suggested that the dominant effect on these modes is caused by the increased ionic size of Pr ion from that of the Y ion (0.90 Å \rightarrow 0.98 Å) [25]. On the other hand, we know that the Raman peak associated with Cu–O stretching vibration (502 cm^{-1}) decreases in frequency when oxygen is removed, while the bending–stretching modes of the Cu–O framework (334 cm^{-1}) harden under the same condition [24, 26]. This implies that the oxygen contents are monotonically increased with the substitution of Pr for Y. Pr addition can increase the oxygen content in the $YBa_2Cu_3O_{7-y}$ system. We suggest that because of the valence change of the Pr ion (as discussed in 3.3) and the different ionic size of Pr versus Y, substitution of Pr for Y directly affects the oxygen content, the shape and distortion of

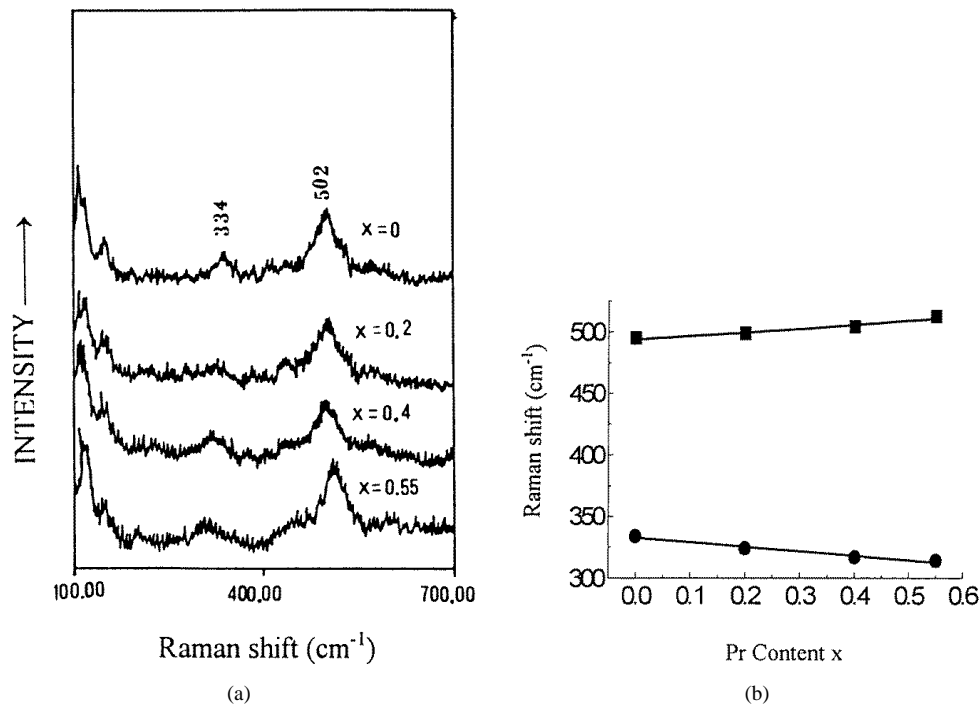


Figure 2. (a) Raman spectra for the samples $Y_{1-x}Pr_xBa_2Cu_3O_{7-y}$; (b) the change of line positions of 334 and 502 cm^{-1} peaks as a function of x .

CuO₂ planes in the Y_{1-x}Pr_xBa₂Cu₃O_{7-y} system, and so causes the change of vibration mode frequency.

Usually, Raman spectra in the range from 100 to 700 cm⁻¹ show the vibrations of Ba, Cu and oxygen and are highly sensitive to the existence of an impurity phase in the YBa₂Cu₃O_{7-y} system. Figure 2(a) shows the Raman spectra for the samples Y_{1-x}Pr_xBa₂Cu₃O_{7-y} ($x = 0.0, 0.2, 0.4, 0.55$). It can be seen that the peaks of the Raman spectra appear at 154, 334 and 502 cm⁻¹, besides the sharp lines below 150 cm⁻¹ which may be due to laser plasma lines and the Raman spectrum of air [22]. The characteristic lines at 154, 334 and 502 cm⁻¹ have been identified as modes having A_g symmetry lattice vibrations for the superconducting phase YBa₂Cu₃O_{7-y} [22–24] suggesting that the samples are the ideal pure Y-123 phase, which agrees with the XRD results. The curves of the line positions of 334 and 502 cm⁻¹ peaks dependent on Pr content are shown in figure 2(b). As seen in figure 2(b), the peak position at 502 cm⁻¹ is a little shifted to a higher frequency while the peak position at 334 cm⁻¹ is shifted to lower frequency with the increase of Pr content. Radousky *et al* suggested that the dominant effect on these modes is caused by the increased ionic size of Pr ion from that of the Y ion (0.90 Å → 0.98 Å) [25]. On the other hand, we know that the Raman peak associated with Cu–O stretching vibration (502 cm⁻¹) decreases in frequency when oxygen is removed, while the bending–stretching modes of the Cu–O framework (334 cm⁻¹) harden under the same condition [24, 26]. This implies that the oxygen contents are monotonically increased with the substitution of Pr for Y. Pr addition can increase the oxygen content in the YBa₂Cu₃O_{7-y} system. We suggest that because of the valence change of the Pr ion (as discussed in 3.3) and the different ionic size of Pr versus Y, substitution of Pr for Y directly affects the oxygen content, the shape and distortion of CuO₂ planes in the Y_{1-x}Pr_xBa₂Cu₃O_{7-y} system, and so causes the change of vibration mode frequency.

3.3. XPS analyses for the samples Y_{1-x}Pr_xBa₂Cu₃O_{7-y} ($0 \leq x \leq 0.55$)

The XPS spectra of the Ba 3d, O 1s and Y 3d core levels are shown in figure 3. It can be found that the Ba 3d core level peaks at about 778.8 eV, as shown in figure 3(a), and is a little shifted to higher binding energies with increasing Pr content. The O 1s core level in figure 3(b) exhibits its major peak at about 528.6 eV with a clear shoulder at about 2–3 eV

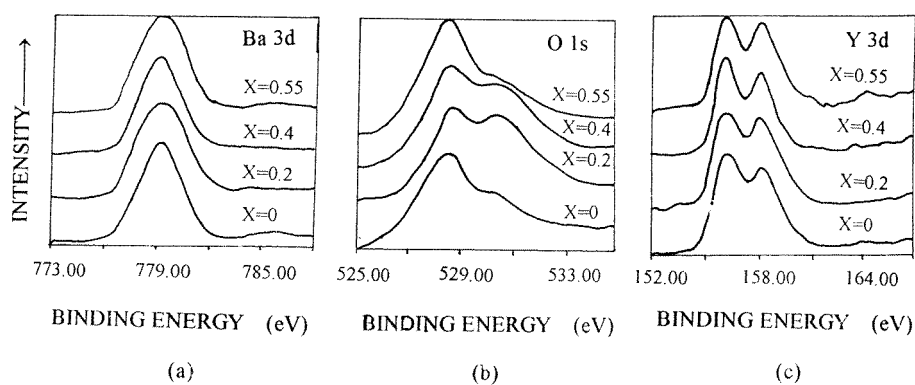


Figure 3. XPS spectra of Y_{1-x}Pr_xBa₂Cu₃O_{7-y} as a function of x for (a) Ba 3d, (b) O 1s and (c) Y 3d core levels.

higher binding energy. It is well known that the shoulder is caused by some sort of oxygen contamination [27]. The doublet peaks of the Y 3d core level XPS appeared at 156.0 and 157.8 eV and showed no shift in peak position with increasing Pr doping, as shown in figure 3(c), but there was a progressive decrease in the intensity of the Y 3d peak with Pr doping. These facts show that the valences of Ba, O and Y ions are basically the same with the change of Pr content x in $Y_{1-x}Pr_xBa_2Cu_3O_{7-y}$, which coincides with the results reported by other groups [20].

The Pr 3d and Cu 2p XPS spectra in the binding energy range from 925.00 to 955.00 eV for $Y_{1-x}Pr_xBa_2Cu_3O_{7-y}$ with $x = 0.0, 0.2, 0.4$ and 0.55 are shown in figure 4. It is known that in this energy range the Cu 2p spectrum consists of the main peaks located at the binding energies of about 933 and 953 eV, and the satellite peak located at 942 eV. On the other hand, the Pr 3d core line also appears in the same energy range. It is difficult to distinguish directly the valence of Pr from the XPS spectra due to the overlap of the Pr 3d core line with the Cu 2p core line. In figure 4, it can be found that the peak position at 932.4 eV is first shifted to a higher binding energy and then to a lower binding energy with the increase of Pr content x . Because the peak position of Cu 2p is fixed, it is suggested that the position change in figure 4 is caused by a profile change of the Pr 3d core line or a change of Pr valence (as shown below). To extract the contribution of the Pr 3d core line to the spectrum of YPrBCO, the Cu 2p spectrum of YBCO was subtracted from the spectrum of YPrBCO. In this subtraction procedure, the intensities of all the spectra of YPrBCO and YBCO were first normalized (based on the heights of the Ba 3d core level peaks at the binding energies of about 778.8 eV) so that the Cu 2p core line and satellite structures did not remain in the spectrum obtained by the subtraction. Then, the complex Pr 3d and Cu 2p XPS spectra of YPrBCO was subtracted by the Cu 2p XPS spectrum of YBCO. In this way, the Pr 3d XPS spectrum can be obtained. Because in this experiment the contents of Ba and Cu for each sample are unchanged (which is confirmed by the WDS of scanning electron microscopy), and the core levels (O 1s, Y 3d, Cu 2p) showed no systematic change in lineshape or binding energy with Pr doping [17–20], the systematic change obtained by the procedure is reliable. The Pr 3d spectra obtained by the above spectrum-subtraction procedures are shown in figure 5. It can be found that there are two peaks located at about 931.8 and 934.4 eV in figure 5. The relative intensities of the two peaks are changed with the change of Pr concentration. Specifically, the intensity of the

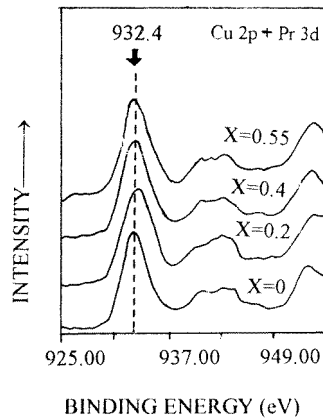


Figure 4. XPS spectra of Pr 3d and Cu 2p of $Y_{1-x}Pr_xBa_2Cu_3O_{7-y}$ as a function of x .

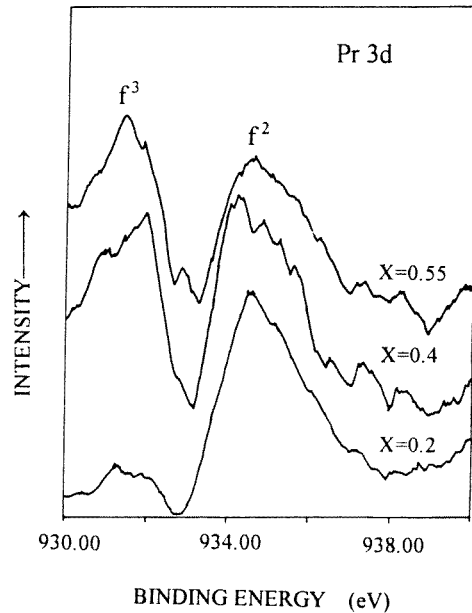


Figure 5. Pr 3d XPS spectra of $Y_{1-x}Pr_xBa_2Cu_3O_{7-y}$ as a function of x , which were extracted after subtraction of the Cu 2p spectra of $YBa_2Cu_3O_{7-y}$.

peak at 931.8 eV increases while the one at 934.4 eV decreases with the increasing of Pr content x .

To characterize the XPS of Pr^{3+} , Ogasawara *et al* [28] have determined the XPS of Pr_2O_3 . The experimental results reveal that there are two peaks (denoted by f^2 and f^3 , respectively) appearing at the binding energies of ~ 935 and ~ 930 eV, respectively. For Pr_2O_3 with Pr^{3+} , the two peak structures are due to the $3d^9 4f^2 \underline{\underline{L}}$ and $3d^9 4f^3 \underline{\underline{L}}$ ($\underline{\underline{L}}$ denotes a ligand hole) final state configurations [29]. On the other hand, according to the analysis of the Pr 3d XPS of PrO_2 with Pr^{4+} ions [29], there are also two peaks appearing in the same region, which correspond to the $3d^9 4f^2 \underline{\underline{L}}$ and $3d^9 4f^3 \underline{\underline{L}}^2$ final states. For both situations, it can be found that the related intensities of the peaks f^2 and f^3 are similar, with a small difference in their positions. Ishii *et al* [30] have checked the Pr 3d XPS spectra of $Pr_{0.8}Bi_{0.2}BaO_3$, Pr_6O_{11} and Pr_2O_3 (as shown in figure 6) with differing relative content of Pr^{3+} and Pr^{4+} ions. Comparing their results, we can see that besides partial repetition of the results of Pr_2O_3 observed by Ogasawara *et al* [28] the related intensities of the f^2 and f^3 peaks are changed with the change in relative content of the Pr^{3+} and Pr^{4+} ions. Specifically, the f^2 peak intensity increases with the content of Pr^{3+} ion increasing while the f^3 peak intensity decreases under the same condition. Thus, the change in relative intensity of f^2 and f^3 peaks can be used to determine the change of the Pr valence. The change of the relative intensities of the two peaks in figure 5 reflects the change of Pr valence. From figure 6, we can obtain that the height ratios of the peaks f^2 and f^3 are 1:0.45 and 1:0.98 for Pr_2O_3 with the Pr^{3+} ion alone and $Pr_{0.8}Bi_{0.2}BaO_3$ with both Pr^{3+} and Pr^{4+} ions, respectively. For YPrBCO, in figure 5 the height ratio of the two peaks at 931.8 and 934.4 eV is changed from about 1:0.26 to 1:1.18 with increasing of Pr content x , which indicates that the Pr valence in YPrBCO is changed with the change of Pr content x . There are two valences of Pr ions in YPrBCO. The Pr valence is a mixed valence of +3 and +4. The relative contents

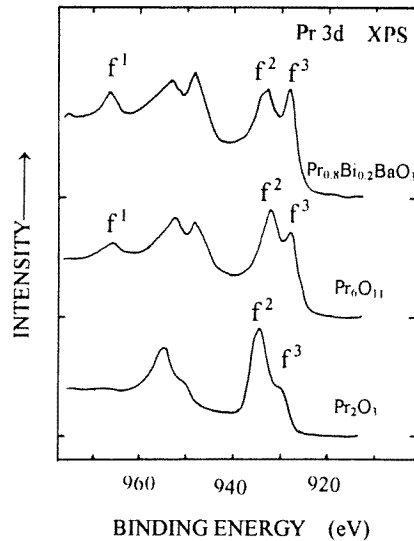


Figure 6. Pr 3d XPS spectra of $\text{Pr}_{0.8}\text{Bi}_{0.2}\text{BaO}_3$, Pr_6O_{11} and Pr_2O_3 (after Ishii *et al* [30]).

of Pr^{3+} ion and Pr^{4+} ion are determined by the total Pr content x . When x is small, the Pr valence in YPrBCO is close to 3+. When x is increased, however, the Pr valence becomes higher. For $\text{PrBa}_2\text{Cu}_3\text{O}_7$, the valence of Pr is mixed with almost equal numbers of Pr^{3+} and Pr^{4+} [32]. This fact is also confirmed by the increase of oxygen content indicated by Raman spectrum analyses (see 3.2). The valence increase of the Pr ion with increase of Pr concentration appears to promote some extra oxygen ion content. It was reported by Booth *et al* from x-ray-absorption fine structure [12] that some extra oxygen atoms around the Pr become disordered and/or distorted and give also an effect on the CuO_2 plane.

In explanation of the suppression of superconductivity in the YPrBCO system, a model of hole filling in the CuO_2 planes is supposed in terms of the mixed valence behaviour of Pr involving a valence close to +4 as witnessed to by specific-heat [5, 6, 13, 14], susceptibility [5, 6], Hall-effect [15] and chemical substitution studies [31]. This appears to be in contradiction with the model of Abrikosov–Gorov-type pair breaking and/or localization of holes in the CuO_2 planes in terms of the hybridization of the 4f electrons of Pr^{3+} with O 2p–Cu 3d electrons in the CuO_2 planes suggested from the high-energy spectrum [9] and x-ray absorption spectroscopy [10–12]. Unfortunately, none of the above-mentioned models allows for a fully consistent interpretation of all experimental data. Moreover, Fink *et al* [9] have determined by EELS that the dopant Pr does not significantly change the total hole density of the YPrBCO system. Our results clearly reveal that in the YPrBCO system the Pr valence is a mixed valence of Pr^{3+} and Pr^{4+} . The relative content of Pr^{4+} to Pr^{3+} increases with increasing Pr concentration. These results support the view that the 4+/hybridization model put forth by Fehrenbacher and Rice [32] is a suitable one for understanding the suppression of superconductivity in the YPrBCO system. According to the 4+/hybridization model, a ligand hole localized on the Pr–O(2)/O(3) band would remove a hole from the conduction band and yield a formal Pr^{4+} site. The strong hybridization between Pr 4f electrons and conduction holes in the CuO_2 planes induces a localization of mobile holes causing the suppression of superconductivity in the YPrBCO system. In addition to this, we suggest that the existence of some extra oxygen atoms around the Pr

(revealed by the Raman spectra in this work and x-ray-absorption fine structure [12]) also produces an effect on the superconductivity by affecting the distortion of the CuO₂ planes. The suppression of the superconductivity in YPrBCO system can then be attributed to the combination of the 4+/hybridization model plus some local distortion of the CuO₂ planes.

4. Conclusion

From analyses of the Y_{1-x}Pr_xBa₂Cu₃O_{7-y} (0 ≤ x ≤ 0.55) system by XRD, Raman spectra and XPS, it is found that the Pr dopant does not change the orthorhombic symmetry of the system. The samples are of ideal pure Y-123 single phase form. The peak positions at 502 and 334 cm⁻¹ of the Raman spectra become shifted for different Pr concentration, which suggests the increase of oxygen content with the substitution of Pr for Y. The changes of oxygen content and the Pr 3d XPS spectra of Y_{1-x}Pr_xBa₂Cu₃O_{7-y} reveal that there are two kinds of valence of Pr ions in YPrBCO. The valence of Pr is changed with the change of Pr content x. The relative content of the Pr³⁺ ion and the Pr⁴⁺ ion are determined by the total Pr content x. The valence of Pr is close to 3+ for small x, and increases as x increases. For PrBa₂Cu₃O₇, the valence of Pr is strongly mixed with almost equal numbers of Pr³⁺ and Pr⁴⁺. The substitution of Pr for Y and the presence of extra oxygen would affect the distortion of the CuO₂ planes. The suppression of superconductivity and the occurrence of semiconductivity can be related to both the valence change of the Pr ions and the distortion of the CuO₂ planes.

Acknowledgments

This project was partly supported by the National Centre for Research and Development on Superconductivity, the National Science Foundation and the National Education Commission of China.

References

- [1] Soderholm L, Zhang K, Hinks D G, Beno M A, Jorgensen J D, Segre C U and Schuller I K 1987 *Nature* **328** 604
- [2] Tang X X, Manthiram A and Goodenough J B 1989 *Physica C* **161** 574
- [3] Dalichaouch Y, Torikachvili M S, Early E A, Lee B W, Seaman C L, Yang K N, Zhou H and Maple M B 1988 *Solid State Commun.* **65** 1001
- [4] Neumeier J J, Bjornholm T, Maple M B, Rhyne J J and Gotaas J A 1990 *Physica C* **166** 191
- [5] Maple M B, Lee B W, Neumeier J J, Nieva G, Paulius L M and Seaman C L 1992 *J. Alloys Compounds* **181** 135
- [6] Kebede A, Jee C S, Schwegler J, Crow J E, Mihalisin T, Myer G H, Salomon R H, Schlottmann P, Kuric M V, Bloom S H and Guertin R P 1989 *Phys. Rev. B* **40** 4453
- [7] Felner I, Yaron U, Nowik I, Bauminger E R, Wolfus Y, Yacoby Y R, Hilscher G and Pillmayr N 1989 *Phys. Rev. B* **40** 6739
- [8] Peng J L, Klavins P, Shelton R N, Radousky H B, Hahn P A and Bernardes L 1989 *Phys. Rev. B* **40** 4517
- [9] Fink J, Nücker N, Romberg H, Alexander M, Maple M B, Neumeier J J and Allen J W 1990 *Phys. Rev. B* **42** 4823
- [10] Soderholm L and Goodman G L 1989 *J. Solid State Chem.* **81** 121
- [11] Horn S, Cai J, Shaheen S A, Jeon Y, Croft M, Chang C L and Den Boer M L 1987 *Phys. Rev. B* **36** 3895
- [12] Booth C H, Bridges F, Boyce J B, Claeson T, Zhao Z X and Cervants P 1994 *Phys. Rev. B* **49** 3432
- [13] Ghamaty S, Lee B W, Neumeier J J, Nieva G and Maple M B 1991 *Phys. Rev. B* **43** 5430
- [14] Nieva G, Ghamaty S, Lee B W, Maple M B and Schuller I K 1991 *Phys. Rev. B* **44** 6999
- [15] Matsuda A, Kinoshita K, Ishii T, Shibata H, Wanatabe T and Yamada T 1988 *Phys. Rev. B* **38** 2910
- [16] Bhadra R *et al* 1988 *Phys. Rev. B* **37** 5142

- [17] Kang J S, Allen J W, Shen Z X, Ellis W P, Yeh J J, Lee B W, Maple M B, Spicer W E and Lindau I 1989 *J. Less-Common Met.* **148** 121
- [18] Wu N J, Xie K, Zhao L H, Zhou Y, Hu D W, Ran Z Y and Zhao Z X 1989 *Solid State Commun.* **69** 615
- [19] Yang I S, Schrott A G and Tsuei C C 1990 *Phys. Rev. B* **41** 8921
- [20] Cohen O, Potter F H, Rastomjee C S and Egdell R G 1992 *Physica C* **201** 58
- [21] Neumeier J J 1990 *PhD Thesis* University of California
- [22] Rosen H, Engler E M, Strand T C, Yu Lee V and Bethune D 1987 *Phys. Rev. B* **36** 726
- [23] Hemley R J and Mao H K 1987 *Phys. Rev. Lett.* **58** 2340
- [24] Thomsen C, Liu R, Bauer M, Wittlin A, Genzel L, Cardona M, Schönher E, Bauhofer W and König W 1988 *Solid State Commun.* **65** 55
- [25] Radousky H B, McCarty K F, Peng J L and Shelton R N 1989 *Phys. Rev. B* **39** 12 383
- [26] Starola M, Krol D M, Weber W, Sunshine S A, Jayaraman A, Kourouklis G A, Cava R J and Rietman E A 1987 *Phys. Rev. B* **36** 850
- [27] Lindberg P A P, Shen Z X, Lindau I, Spicer W E, Mitzi D B and Kapitulnik A 1989 *Solid State Commun.* **72** 575
- [28] Ogasawara H, Kotani A, Potze R, Sawatzky G A and Thole B T 1991 *Phys. Rev. B* **44** 5465
- [29] Kotani A and Ogasawara H 1992 *J. Electron Spectrosc. Relat. Phenom.* **60** 257
- [30] Ishii H, Jokura K, Kataura H and Hanyu T 1995 *Japan. J. Appl. Phys.* **34** L814
- [31] Neumeier J J, Bjornholm T, Maple M P and Schuller I K 1989 *Phys. Rev. Lett.* **63** 2516
- [32] Fehrenbacher R and Rice T M 1993 *Phys. Rev. Lett.* **70** 3471